Junction Conditions for Hamilton–Jacobi Equations for Solving Real-Time Traffic Flow Problems

LINFENG ZHANG[1,2,3], **HONGFEI JIA**[1], **NICOLAS FORCADEL**[2], **AND BIN RAN**[3]

[1]School of Transportation, Jilin University, Changchun 130012, China
[2]INSA de Rouen, Normandié Université, Laboratory de Mathématiques de I'INSA-LMI (EA 3226 - FR CNRS 3335), 76801 St. Etienne du Rouvray, France
[3]Department of Civil and Environmental Engineering, University of Wisconsin–Madison, Madison, WI 53706, USA

Corresponding author: Hongfei Jia (jiahf@jlu.edu.cn)

ABSTRACT In this paper, we propose junction conditions for discontinuities due to local perturbation, diverging, merging, and multi-in-multi-out junctions. Traffic flows on junctions can be described by a system of coupled Hamilton-Jacobi equations. At their connection points, it is necessary to propose appropriate junction conditions to close the system. Then, we provide an effective numerical method to compute approximate solutions to these Hamilton-Jacobi equations on junctions. The numerical boundary conditions to close the Hamilton-Jacobi system are also proposed. Numerical tests demonstrate the effectiveness of both the proposed junction conditions and the numerical method.

INDEX TERMS Hamilton-Jacobi equation, junction condition, traffic flow, local perturbation, macroscopic model.

I. INTRODUCTION

Many traffic flow models have recently been designed. These models are mainly used to study the temporal and spatial distributions of traffic density and the driving habits of car drivers, particularly by governments or their departments to design traffic facilities or to provide references for the construction of roads [1], [2]. Generally, the existing models can be divided into two types: macroscopic traffic models and microscopic models. Research on the macroscopic models began with the LWR model of Lighthill and Whitham [3] and Richards [4]. This LWR model describes the temporal-spatial distribution of traffic density. It is a system of partial differential equations (PDEs). We also refer to the book by Garavello and Piccoli [5] and the references therein for a good introduction. Moreover, note that macroscopic models can also be described in terms of the cumulative number of vehicles, i.e., the primitive of the density (see, for example, [6]). This approach leads to the Hamilton-Jacobi

The associate editor coordinating the review of this article and approving it for publication was Zhengbing He.

equations, which have been studied on networks very recently by Imbert and Monneau [7]. Regarding the microscopic traffic flow models, Pipes [8] studied the car-following model almost half a century ago, which described the processes by which drivers follow each other in traffic streams [9]. Later, there were some extensions to this model by Helly, Kometani and Sasaki [10] and Gazis *et al.* [11]. Additionally, there are many microscopic traffic models such as [12], [13]. One can find some references from the review paper [9].

To compute the macroscopic traffic network, the Cell Transmission Method and Link Transmission Method can be used. We can refer to the papers [14], [15] for the Cell Transmission Method and to [16], [17] for the Link Transmission Method. The second method can be derived from the Hamilton-Jacobi system, which only discretizes the time. For the Hamilton-Jacobi approach, the traffic can be divided into two parts: the homogeneous roads and the nodes linking them. One can refer to [18]–[20]. The roads can be described by Hamilton-Jacobi equations, and we should provide junction conditions at the nodes to close the traffic network problem. For the classical Hamilton-Jacobi equations,

there are many numerical methods, such as ENO [21] and WENO [22], to compute the discontinuities such as shock waves. Numerical methods are also used in [23], [24] to compute the Hamilton-Jacobi system. The goal of this paper is to propose different types of junctions and provide an effective numerical method for computing junctions. The following junction conditions are generally the main types at the nodes: local perturbation, bifurcation, merging and multi-in-multi-out, which have increasing complexity.

Local perturbations in traffic flows, such as road obstacles, curves and even braking, such as at traffic lights, are very common. It is easy to use a microscopic traffic model to describe the local deceleration simply by multiplying by an attenuation factor. In fact, the corresponding macroscopic traffic model is hard to write. If a penalty term or a viscosity term is added to the right side of the equation, the properties of the equation will change, and the simulation will be unnatural. Therefore, it is difficult but important to propose a macroscopic model with local perturbations. Notably, this has been done in [25], where the authors obtain a macroscopic model with a junction condition from a microscopic model with a local perturbation.

According to this idea, we must construct more complex junctions. The junctions should satisfy the following conditions. First, the traffic generally encounters a local perturbation (flux limiter) at the nodes. Second, the traffic distribution should be set. In addition, it is also very important that the total number of traffic flows remain unchanged. The proposed numerical method should also retain these properties.

The goal of this paper is to propose junction conditions for local perturbation, bifurcation, merging and multi-in-multi-out nodes on a network. Let us refer to the works [26], [27] for some finite difference schemes to solve this type of equations.

The model is proposed in Section 2, and the numerical method for this system is shown in Section 3. We present several numerical tests to demonstrate the effectiveness of the proposed junction conditions and numerical methods in Section 4. At the end of this paper, we provide some conclusions and remarks.

II. TRAFFIC FLOW MODEL POSED ON A JUNCTION

In fact, the entire transportation network can be roughly divided into two parts. One part is the uniform road, which can be described by the Hamilton-Jacobi equations. The other part is the nodes that link these roads. Junction conditions are used to model traffic flows through nodes. We consider junction conditions to be dynamic boundary conditions for the Hamilton-Jacobi equations. These conditions provide the distribution rules for upstream fluxes at the nodes. In this section, we describe the junction conditions for various nodes in detail.

We use the following settings: there are M incoming roads and N outgoing roads posed on the junction point O shown in Fig. 1. The set of load numbers is defined as $Q = \{-M, -M+1, \ldots, -1, 1, \ldots, N-1, N\}$.
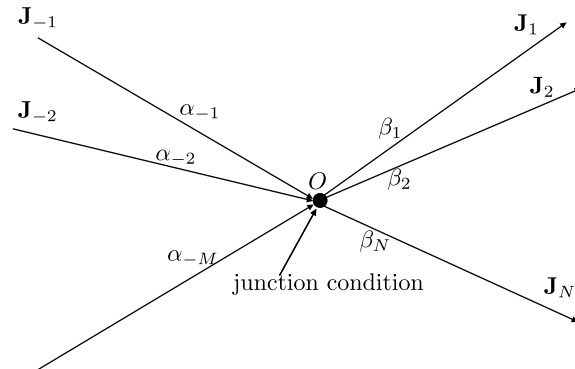

FIGURE 1. Junction approach for traffic flow networks.

The M-in lane is defined on

$$\mathrm{J}_i = (-\infty, 0] \cdot \mathbf{e}^i, \quad \mathrm{J}_i^* = \mathrm{J}_i \backslash \{0\}, \quad i = -M, \ldots, -1. \quad (1)$$

The N-out lane after the junction is defined on

$$\mathrm{J}_i = [0, +\infty) \cdot \mathbf{e}^i, \quad \mathrm{J}_i^* = \mathrm{J}_i \backslash \{0\}, \quad i = 1, \ldots, N, \quad (2)$$

with linearly independent unit vector set $\{\mathbf{e}^i | i \in Q\}$.

The traffic is defined on

$$\mathrm{J} = \bigcup_{i \in Q} \mathrm{J}_i. \quad (3)$$

and the junction point is

$$\{x = 0\} = \bigcap_{i \in Q} \mathrm{J}_i. \quad (4)$$

We assume that all vehicles follow the ODE systems on each road J_i according to Fig. 1,

$$\dot{U}_j = V_i(U_{j+1}(t) - U_j(t)) * \phi(t, U_j(t)). \quad (5)$$

Functions $V_i(h)$ and $\phi(t, x)$ satisfy the following assumptions
- $V_i \colon \mathbb{R} \to \mathbb{R}^+$ is Lipschitz continuous and non-negative.
- V_i is non-decreasing on $\mathbb{R}$.
- There exists a $h_i \in (0, +\infty)$ such that for all $h < h_i$, $V_i(h) = 0$.
- There exists a $h_{max}^i \in (h_i, +\infty)$ such that for all $h > h_{max}^i$, $V_i(h) = V_i(h_{max}^i) = V_{max}^i$.
- There exists a real $p_i \in [-k_i, 0)$ such that the function $p \mapsto pV(-1/p)$ is decreasing on $[-k_i, p_i)$ and increasing on $[p_i, 0)$, where $k_i := 1/h_i$.
- The function $\mathbb{R} \times \mathbb{R} \to [0, 1]$ is Lipschitz continuous and there exist $r > 0$ such that $\phi(t, x) = 1$ for $|x| > r$.

Following [25] and [28], the macroscopic model on J is a Hamilton-Jacobi model posed on a junction

$$\begin{cases} u_t^i + H_i(u_x^i) = 0 & \text{for} \quad x \in \mathrm{J}_i^*. \\ u_t^i + F_A^i\left(u_x^i(t, 0^-), u_x^i(t, 0^+)\right) = 0 & \text{for } x = 0 \\ u(0, x) = u_0(x) & \text{for } x \in \mathbb{R}, \end{cases} \quad (6)$$

where u is the distribution function, and the car density ρ reads as

$$\rho(x, t) = -u_x(x, t) \quad x \neq 0. \quad (7)$$

$A \leq 0$ is a constant called the flux limiter, $H_i, i \in Q$ are defined by

$$H_i(p) = -V_i \left(\frac{-1}{p}\right) |p| \quad \text{for } -k_i \leq p < 0 \qquad (8)$$

with

$$H_i^-(p) = \begin{cases} H_i(p) & \text{if } p \leq p_i \\ H_i(p_i) & \text{if } p \geq p_i \end{cases} \qquad (9)$$

and

$$H_i^+(p) = \begin{cases} H_i(p_0) & \text{if } p \leq p_i \\ H_i(p) & \text{if } p \geq p_i \end{cases} \qquad (10)$$

Here, the parameter p indicates the opposite of traffic density. Fig. 2 shows the diagram of functions $H_i(p)$, $H_i^+(p)$ and $H_i^-(p)$. The function $H_i(p)$ has a minimum point H^i at $p = p_i$, $H_i^+(p)$ is an increasing function, and $H_i^-(p)$ is a decreasing function.
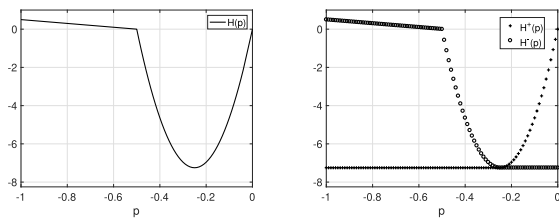

FIGURE 2. The diagram of the functions $H_i(p)$ (left) and $H_i^+(p)$ and $H_i^-(p)$ (right).

As we discuss above, the traffic flow can be described as Hamilton-Jacobi equations on each lane, and we should provide an effective junction condition on the junction point $x = 0$. In this way, the entire traffic network is constructed. In this section, we propose each node junction condition from simple to difficult.

A. LOCAL PERTURBATION

First, we begin with a simple junction problem, which is a road with a local perturbation at the origin point, where we set $M = N = 1$.

The junction condition on $x = 0$ reads as

$$u_t^i + F_A(u_x^i(t, 0^-), u_x^i(t, 0^+)) = 0, \quad i = -1, 1, \quad (11)$$

and F_A is defined on $x = 0$ as

$$F_A(p_-, p_+) = \max(A, H_{-1}^+(p_-), H_1^-(p_+)) \qquad (12)$$

The flux limiter A is defined in $[A_0, 0]$, and

$$A_0 = \max\left(\min_{p \in \mathbb{R}}\left(H_{-1}^+(p)\right), \min_{q \in \mathbb{R}}\left(H_1^-(q)\right)\right) \qquad (13)$$

as a local perturbation around the junction point.

Theorem 1 (Maximum Principle): Let $u(x, t)$ be a solution to Eq. (6) and the junction condition (11) with initial data $u(x, 0) = u_0(x)$. If u_0 is Lipschitz continuous and satisfies

$$\begin{cases} -k_{-1} \leq (u_0)_x \leq 0 & \text{for } x < 0 \\ -k_1 \leq (u_0)_x \leq 0, & \text{for } x > 0 \end{cases} \qquad (14)$$

then, we have for all $t > 0$ that

$$\begin{cases} -k_{-1} \leq u_x \leq 0 & \text{for } x < 0 \\ -k_1 \leq u_x \leq 0, & \text{for } x > 0 \end{cases} \qquad (15)$$

Proof: Based on the [25], we give the following ideas to prove the boundedness:
Set

$$\Omega = \{(t, x, y) \in [0, T) \times \mathbb{R}, x \geq y\}$$

We introduce,

$$M = \sup_{(t,x,y) \in \Omega} \{u(t, x) - u(t, y)\}. \qquad (16)$$

We want to prove that $M \leq 0$. We argue by contradiction and assume that $M > 0$. For any $\eta, \alpha > 0$, small parameters, we define

$$\varphi(t, x, y) = u(t, x) - u(t, y) - \frac{\eta}{T - t} - \alpha x^2 - \alpha y^2. \qquad (17)$$

Then, we have that

$$\varphi(t, x, y) \leq u_0(x) - u_0(y) + 2M_0 k_0 T - \alpha(x^2 + y^2)$$
$$\leq -\alpha(x^2 + y^2) + +2M_0 k_0 T, \qquad (18)$$

where we used assumption $-k_{-1} \leq (u_0)_x \leq 0$ for the second inequality. Therefore, we have

$$\lim_{|x|, |y| \to +\infty} \varphi(t, x, y) = -\infty. \qquad (19)$$

Since φ is upper-semi continuous, it reaches a maximum at a point that we denote by $(\bar{t}, \bar{x}, \bar{y}) \in \Omega$. Classically we have for η and α small enough,

$$\begin{cases} 0 < \frac{M}{2} \leq \varphi(\bar{t}, \bar{x}, \bar{y}), \\ \alpha|\bar{x}|, \alpha|\bar{y}| \to 0 & \text{as } \alpha \to 0. \end{cases} \qquad (20)$$

$\bar{t} > 0$ and $\bar{x} > \bar{y}$. By contradiction, assume first that $\bar{t} = 0$. Then, we have

$$\frac{\eta}{T} < u_0(\bar{x}) - u_0(\bar{y}) \leq 0, \qquad (21)$$

where we used that u_0 is non-increasing, and we get a contradiction. The fact that $\bar{x} > \bar{y}$, comes directly from the fact that $\varphi(\bar{t}, \bar{x}, \bar{y}) > 0$.

By doing a duplication of the time variable and passing to the limit in this duplication parameter, we get that

$$\frac{\eta}{(T - \bar{t})^2} \leq \bar{M}[u(\bar{(t)}, y)](\bar{y}) \cdot |2\alpha\bar{y}| \cdot \phi(\bar{t}, \bar{y})$$
$$- \bar{M}[u(\bar{(t)}, x)](\bar{x}) \cdot |2\alpha\bar{x}| \cdot \phi(\bar{t}, \bar{x})$$
$$\leq 2M_0 \alpha(|\bar{x}| + |\bar{y}|), \qquad (22)$$

passing to the limit as α goes to 0, we obtain a contradiction.

On the other hand, we introduce

$$M = \sup_{(t,x,y) \in \Omega} \{u(t, x) - u(t, y) - k_0(x - y)\}. \qquad (23)$$

We want to prove that $M \leq 0$. We argue by contradiction and assume that $M > 0$.

For any $\eta, \alpha > 0$, small parameters, we define

$$\varphi(t, x, y) = u(t, y) - u(t, x) - \frac{\eta}{T - t}$$
$$-\alpha x^2 - \alpha y^2 - k_0(x - y). \quad (24)$$

Then, we have that

$$\varphi(t, x, y) \leq u_0(y) - u_0(x) + 2M_0 k_0 T$$
$$- \alpha(x^2 + y^2) - k_0(x - y)$$
$$\leq -\alpha(x^2 + y^2) + +2M_0 k_0 T, \quad (25)$$

Therefore we have

$$\lim_{|x|, |y| \to +\infty} \varphi(t, x, y) = -\infty. \quad (26)$$

Using the fact that φ is upper-semi continuous we deduce that φ reaches a maximum at a finite point that we denote $(\bar{t}, \bar{x}, \bar{y}) \in \Omega$. Classically we have for η and α small enough,

$$\begin{cases} 0 < \dfrac{M}{2} \leq \varphi(\bar{t}, \bar{x}, \bar{y}), \\ \alpha|\bar{x}|, \alpha|\bar{y}| \to 0 \qquad \text{as } \alpha \to 0. \end{cases} \quad (27)$$

$\bar{t} > 0$ and $\bar{x} > \bar{y}$. By contradiction, assume first that $\bar{t} = 0$. Then, we have

$$\frac{\eta}{T} < u_0(\bar{x}) - u_0(\bar{y}) \leq 0, \quad (28)$$

which is a contradiction. Hence $\bar{t} > 0$. Using that $\varphi(\bar{t}, \bar{x}, \bar{y}) > 0$, we deduce that $\bar{x} \geq \bar{y}$.

By duplicating the time variable and passing to the limit we have -uthat there exists two real numbers a, b, such that $(a, -k_0 + 2\alpha\bar{y}) \in \bar{D}^+ u(\bar{t}, \bar{y}, (b, -k_0 + 2\alpha\bar{x}) \in \bar{D}^+ u(\bar{t}, \bar{x}$ and

$$a - b = \frac{\eta}{(T - \bar{t})^2}. \quad (29)$$

we get

$$a + M[u(t, \bar{y})](\bar{y}) \cdot \phi(\bar{t}, \bar{y}) \cdot | - k_0 + 2\alpha\bar{y}| \leq 0. \quad (30)$$

We claim

$$M[u(t, \bar{y})](\bar{y}) = \int_{\mathbb{R}} J(z) E(u(\bar{t}, \bar{y} + z) - u(\bar{t}, \bar{y})) dz$$
$$- \frac{3}{2} V_{max}$$
$$= 0 \quad (31)$$

Indeed, let $z \in (h_0, h_{max}]$. If $\bar{y} + z \geq \bar{x}$, using that u is non-increasing in space according above, we get

$$u(\bar{t}, \bar{y} + z) - u(\bar{t}, \bar{y}) \leq u(\bar{t}, \bar{x}) - u(\bar{t}, \bar{y})$$
$$\leq -k_0(\bar{x} - \bar{y}) \leq 0 \quad (32)$$

If $\bar{y} + z < \bar{x}$, using the fact that $\varphi(\bar{t}, \bar{x}, \bar{y} + z) \leq \varphi(\bar{t}, \bar{x}, \bar{y})$, for α small enough, we obtain

$$u(\bar{t}, \bar{y} + z) - u(\bar{t}, \bar{y}) \leq -k_0 z + \alpha(2z\bar{y} + z^2)$$
$$\leq -k_0 z + (2h_{max}\bar{y} + h_{max}^2) \leq 0 \quad (33)$$

This implies that we have for all $z \in (h_0, h_{max}]$,

$$E(u(\bar{t}, \bar{y} + z) - u(\bar{t}, \bar{y})) = \frac{3}{2}. \quad (34)$$

Injecting this in the non-local term, we deduce the claim.

Finally, the fact that $u_t \geq 0$ implies that $a, b \geq 0$. Therefore, inequality (30) implies $a = 0$. Using (29), we obtain

$$\frac{\eta}{T^2} \leq 0, \quad (35)$$

which is a contradiction. $\square$

The Hamilton-Jacobi equations with a junction condition actually describe a deceleration behaviour (local perturbation) of the traffic flow at the node. The flux limiter A reflects the local perturbation in the microscopic model. Many types of transportation nodes that we encounter, such as bifurcation and merging, have such deceleration behaviour. We use this approach as a basis to build more complex junction conditions.

B. BIFURCATION CONDITION

In this subsection, the analytical bifurcation condition is introduced. We first define the setting of the problem according to Fig.3.
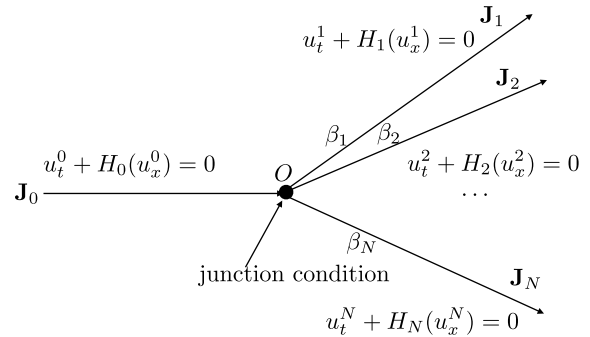
FIGURE 3. Schematic representation of the bifurcation problem.

We give the junction condition as

$$\begin{cases} u_t^i + \beta_i F_A = 0 & \text{for } x = 0, \ i = 1, \dots, N \\ u_t^{-1} + F_A = 0 & \text{for } x = 0. \end{cases} \quad (36)$$

Here, the percentage $\beta_i \geq 0$ and $\sum \beta_i = 1$. F_A is defined on $x = 0$ as

$$F_A = \max \left(A, H_{-1}^+(u_x^{-1}), \max_{i=1}^{N} \left(\frac{H_i^-(u_x^i)}{\beta_i} \right) \right). \quad (37)$$

The flux limiter A is defined in the closed interval $[A_0, 0]$, and

$$A_0 = \max \left(\min_{p \in \mathbb{R}} \left(H_{-1}^+(p) \right), \max_{i=1}^{N} \left(\frac{\min_{q \in \mathbb{R}} \left(H_i^-(q) \right)}{\beta_i} \right) \right), \quad (38)$$

as a local perturbation around the junction point.

Theorem 2: Set $u^i(t, x)$ is a solution to Eq.(6) with junction condition (36) and initial data $u^i(0, x) = u_0^i(x)$. If u_0^i is Lipschitz continuous and satisfies

$$-k_i \leq (u_0^i)_x \leq 0, \quad x \in \mathbf{J}_i^*, \ i = -1, 1, 2, \dots, N, \quad (39)$$

then, we have for all $t > 0$ that

$$-k_i \leq u_x^i \leq 0, \quad x \in \mathbf{J}_i^*, \ i = -1, 1, 2, \dots, N. \quad (40)$$
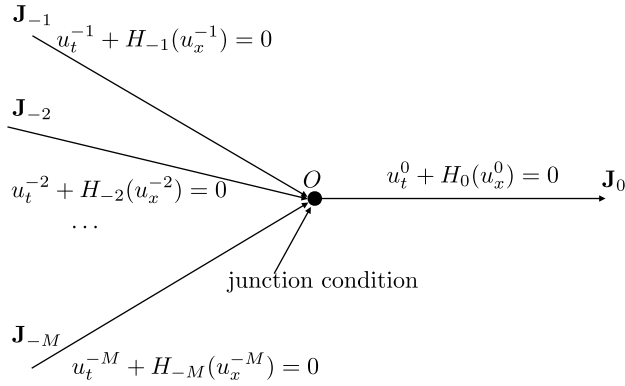
FIGURE 4. Schematic representation of the merging problem.

C. MERGING CONDITION

In this subsection, we present the merging problem with $M > 1$ and $N = 1$. The first part presents the merging as a zipper. Then, we show the merging problem on demand.

Merging as a zipper is where a certain percentage of the cars before the junction point strictly flow into the i-st lane. The percentages are as follows:

$$\alpha_i \in (0, 1], \quad \sum_{i=1}^{N} \alpha_i = 1. \tag{41}$$

This junction condition is

$$\begin{cases} u_t^i + \alpha_i F_A = 0 & \text{for } i < 0 \\ u_t^1 + F_A = 0. \end{cases} \tag{42}$$

Here, F_A is defined on $x = 0$ as

$$F_A = \max\left(A, \max_{i=1}^{N}\left(\frac{H_i^+(u_x^i)}{\alpha_i}\right), H_1^-(u_x^1)\right). \tag{43}$$

The flux limiter A is defined in the closed interval $[A_0, 0]$, and

$$A_0 = \max\left(\max_{i=1}^{N}\left(\frac{\min_{p\in\mathbb{R}}\left(H_i^+(p)\right)}{\alpha_i}\right), \min_{q\in\mathbb{R}}\left(H_1^-(q)\right)\right). \tag{44}$$

However, this situation is only established when the traffic is relatively large. In extreme cases, if one lane's flux is zero, all the remaining lanes will be blocked at the junction point because they should strictly wait for the cars from the lane with zero flux. We will show a numerical test in the next section.

Another junction condition for merging that we present is that the percentage is defined as the flux.

$$\begin{cases} u_t^i + \dfrac{H_j^+(u_x^j)}{\min\left(\sum_{j=-M}^{-1}\left(H_j^+(u_x^j)\right), b\right)}F_A = 0 & \text{for } i < 0 \\ u_t^1 + F_A = 0. \end{cases} \tag{45}$$

Here, b simply takes a very small negative value (for example, $b = -10^{-10}$) to avoid dividing by 0, and F_A is defined on

$x = 0$ as

$$F_A = \max\left(A, \sum_{i=-M}^{-1}\left(H_i^+(u_x^i)\right), H_1^-(u_x^1)\right), \quad x = 0. \tag{46}$$

The flux limiter A is a number is defined in the closed interval $[A_0, 0]$, and

$$A_0 = \max\left(\sum_{i=-M}^{-1}\left(\min_{p\in\mathbb{R}}\left(H_i^+(p)\right)\right), \min_{q\in\mathbb{R}}\left(H_1^-(q)\right)\right). \tag{47}$$

Theorem 3: Set $u^i(t, x)$ is a solution to Eq.(6) with junction condition (42) or (45) and initial data $u^i(0, x) = u_0^i(x)$. If u_0^i is Lipschitz continuous and satisfies

$$-k_i \le (u_0^i)_x \le 0, \quad x \in \mathbf{J}_i^*, \ i = -M, \dots, -1, 1, \tag{48}$$

then, we have for all $t > 0$ that

$$-k_i \le u_x^i \le 0, \quad x \in \mathbf{J}_i^*, \ i = -M, \dots, -1, 1. \tag{49}$$

For more complicated merging cases, we can combine the above two types of junction conditions. For example, we can choose the first junction in the case of relatively large flux traffic and choose the second case for a smaller one. We do not describe these cases here as they are beyond the scope of this article.

D. MULTI-IN-MULTI-OUT CONDITION

In this subsection, we propose a junction condition based on the work [28]. There are M incoming roads and N outgoing roads posed on the junction point O shown in Fig. 5.
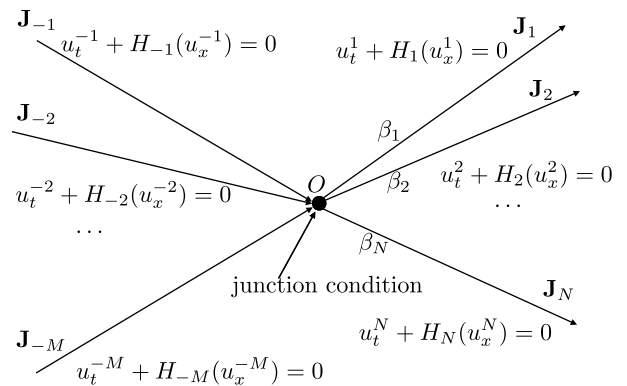

FIGURE 5. Schematic representation of the bifurcation problem.

The equation on the junction point is

$$\begin{cases} u_t^i + \dfrac{H_i^-(u_x^i)}{\left(\sum_{j=-M}^{-1}\left(H_j^-(u_x^j)\right), b\right)}F_A = 0 & \text{for } i < 0 \\ u_t^i + \beta_i F_A = 0 & \text{for } i > 0. \end{cases} \tag{50}$$

Here, b simply takes a very small negative value, as we discuss above, and F_A is defined on $x = 0$ as

$$F_A = \max\left(A, \sum_{i=-M}^{-1}\left(H_i^+(u_x^i)\right), \max_{i=1,\dots,N}\left(\frac{H_i^-(u_x^i)}{\beta_i}\right)\right). \tag{51}$$

The flux limiter A is defined in the closed interval $[A_0, 0]$, and

$$A_0 = \min \left(\left(\sum_{i=-M}^{-1} \left(\min_{p \in \mathbb{R}} \left(H_i^+(p) \right) \right) \right)^{-1}, \min_{q \in \mathbb{R}, i=1}^{N} \left(\frac{H_i^-(q)}{\beta_i} \right) \right).$$
(52)

Theorem 4 (Maximum Principle): Let $u^i(x, 0)$ be a solution to Eq. (6) with junction condition (50) and initial data $u^i(x, 0) = u_0^i(x)$. If u_0^i is Lipschitz continuous and satisfies

$$\begin{cases} -k_1 \le (u_0)_x \le 0 & x \in \mathbf{J}_i, \ i = -M, \dots, -1, \\ -k_2 \le (u_0)_x \le 0 & x \in \mathbf{J}_i, \ i = 1, \dots, N, \end{cases}$$
(53)

then, we have for all $t > 0$ that

$$\begin{cases} -k_1 \le u_x \le 0 & x \in \mathbf{J}_i^*, \ i = -M, \dots, -1, \\ -k_2 \le u_x \le 0 & x \in \mathbf{J}_i^*, \ i = 1, \dots, N. \end{cases}$$
(54)

To summarize, we use the Hamilton-Jacobi equations to calculate the straight roads and use the junction conditions to connect these Hamilton-Jacobi equations. Then, the traffic flow problem is closed.

There exist a unique continuous (relaxed) viscosity solution $u(t, x)$ satisfy the Hamilton-Jacobi equations (6) with junction conditions (11), (36), (42), (45), or (50). In the special case of convex Hamiltonians H_i with different minimum values, problem (6) can be considered as the Hamilton-Jacobi-Bellman equation, see for instance [28] when $A = \infty$. In this case, existence and uniqueness of viscosity solutions have been established either with a very rigid method [28] based on an explicit Oleinik-Lax formula. For $A < 0$, the mathematical prove progress can be found in ([29], Theorem 1.6).

In Section IV, we test these junction conditions and show their effectiveness.

III. NUMERICAL METHODS
In this section, we present a numerical method for solving the Hamilton-Jacobi system with the different junction conditions. Then, we show the positive definiteness and boundedness of the proposed methods. Finally, the boundary conditions and initial conditions are also proposed.

A. NUMERICAL METHODS FOR HAMILTON-JACOBI EQUATIONS ON $\mathbf{J}_i^*$
In the above discussion, we note that the Hamilton-Jacobi equations are used to characterize the dynamic behaviour of traffic in uniform lanes and junction conditions are used to describe information of the nodes. Let us first discuss the numerical method of the Hamilton-Jacobi equations on $\mathbf{J}_i^*$.

Taking a traffic flow problem with a single junction condition on the origin as an example, the number set of the road

is given by

$$Q = \{-M, \dots, -1, 1, \dots, N\}.$$

In particular, $M = N = 1$ is a local perturbation problem, $M = 1, N > 1$ is a bifurcation problem, and $M > 1, N = 1$ is a merging problem.

On the roads $\mathbf{J}_i^*, i \in Q$, the distribution functions u^i are continuous and differentiable. Set

$$m^i(x, t) = u_x^i(x, t), \quad x \in \mathbf{J}_i^*, i \in Q \ t > 0.$$

$m^i(x, t)$ satisfies conservation laws

$$m_t^i + H_i(m)_x^i = 0 \quad x \in \mathbf{J}_i^*, i \in Q, \ t > 0.$$
(55)

We select Δx as the length of the space grid and Δt as the time step. Let

$$x_j^i = j \Delta x \cdot \mathbf{e}^i, \quad t^n = n \Delta t.$$

Then, we approximate $u^i(x, t)$ on the integral point as

$$u_j^{i,n} = u(x_j^i, t^n), \quad i \in Q, j \in \mathbb{Z}, n \in \mathbb{N},$$
(56)

and $m^i(x, t)$ on the half integral space point as

$$m_{j+\frac{1}{2}}^{i,n} = m(x_{j+\frac{1}{2}}^i, t^n), \quad i \in Q, j \in \mathbb{N}, n \in \mathbb{N}.$$
(57)

The relation between u_j^n and $m_{j+\frac{1}{2}}^n$ is given by

$$m_{j+\frac{1}{2}}^{i,n} = \frac{u_{j+1}^{i,n} - u_j^{i,n}}{\Delta x}.$$
(58)

Then, the numerical scheme for computing the Hamilton-Jacobi equations on $\mathbf{J}_i^*$ reads as in (59), as shown at the bottom of this page, where $i \in Q, j \in \mathbb{Z}$ and $n \in \mathbb{N}$.

This scheme should follow the Courant-Friedrichs-Lewy (CFL) condition, which reads as

$$\lambda \cdot \max_{i \in Q} \left(\max_{-k_i \le x \le 0} |H_i'(x)| \right) \le 1$$
(60)

where $\lambda = \Delta t / \Delta x$.

B. NUMERICAL METHODS ON THE JUNCTION POINT
The junction condition can be written in the following form uniformly

$$\begin{cases} u_t^i + \tilde{\alpha}_i F_A = 0 & \text{for } x = 0, \ i = -M, \dots, -1 \\ u_t^i + \beta_i F_A = 0 & \text{for } x = 0, \ i = 1, \dots, N. \end{cases}$$
(61)

where β_i are the given constants

$$\tilde{\alpha}_i \in [0, 1], \quad \beta_i \in [0, 1].$$

$$u_j^{i,n+1} = \frac{u_{j+1}^{i,n} + u_{j-1}^{i,n}}{2} - \frac{\Delta t}{2} \left(H_i \left(\frac{u_{j+1}^{i,n} - u_j^{i,n}}{\Delta x} \right) - H_i \left(\frac{u_j^{i,n} - u_{j-1}^{i,n}}{\Delta x} \right) \right),$$
(59)

$$F_A^n = \max\left(A, \sum_{i=-M}^{-1}\left(H_i^+\left(\frac{u_0^{i,n} - u_{-1}^{i,n}}{\Delta x}\right)\right), \max_{i=1,\dots,N}\left(\frac{1}{\beta_i}H_i^-\left(\frac{u_1^{i,n} - u_0^{i,n}}{\Delta x}\right)\right)\right). \tag{66}$$

and

$$\sum_{-M}^{-1}\tilde{\alpha}_i = \sum_{1}^{N}\beta_i = 1. \tag{62}$$

If the merging problem is similar to a zipper, $\tilde{\alpha}_i = \alpha_i$ is a given constant. If the merging progress depends on the flux,

$$\tilde{\alpha}_i = \frac{H_i^-(u_x^i)}{\left(\sum_{j=-M}^{-1}\left(H_j^-(u_x^j)\right), b\right)}, \quad x = 0. \tag{63}$$

The numerical scheme for Eq. (61) reads as

$$\begin{cases} \dfrac{u_0^{i,n+1} - u_0^{i,n}}{\Delta t} + \tilde{\alpha}_i^n F_A^n = 0 & \text{for } i < 0, \ n > 0, \\[2mm] \dfrac{u_0^{i,n+1} - u_0^{i,n}}{\Delta t} + \beta_i F_A^n = 0 & \text{for } i > 0, \ n > 0, \end{cases} \tag{64}$$

where $\tilde{\alpha}_i^n = \alpha_i$ for zipper merging or

$$\tilde{\alpha}_i^n = \frac{H_i^-\left(\frac{u_0^{i,n} - u_{-1}^{i,n}}{\Delta x}\right)}{\left(\sum_{j=-M}^{-1}\left(H_j^-\left(\frac{u_0^{i,n} - u_{-1}^{i,n}}{\Delta x}\right)\right), b\right)}, \tag{65}$$

for another type of merging.

The numerical scheme for computing F_A^n is shown in (66), as shown at the top of this page.

Theorem 5 (Discrete Maximum Principle): Let $\lambda = \Delta t/\Delta x$. If Δt and Δx satisfy the CFL condition (60) and the initial data satisfy

$$-k_i \le m_{j+\frac{1}{2}}^{i,0} \le 0, \tag{67}$$

with the numerical scheme (59) with the junction condition (64) and considering the relationship (58), then, we have for every $n \in \mathbb{N}^+$,

$$-k_i \le m_{j+\frac{1}{2}}^{i,n} \le 0. \tag{68}$$

Proof: We should prove that if $-k_i \le m_{j+\frac{1}{2}}^{i,n} \le 0$, then, $-k_i \le m_{j+\frac{1}{2}}^{i,n+1} \le 0$.

If $i < 0$ and $j < 0$, we have

$$m_{j+\frac{1}{2}}^{i,n+1} = \frac{1}{2}\left(m_{j+\frac{3}{2}}^{i,n} + m_{j-\frac{1}{2}}^n\right) + \frac{\lambda}{2}\left(H_i\left(m_{j+\frac{3}{2}}^{i,n}\right) - H_i\left(m_{j-\frac{1}{2}}^{i,n}\right)\right). \tag{69}$$

Set the function

$$y_1 = \frac{1}{2}(x_1 + x_2) + \frac{\lambda}{2}\left(H_i(x_1) - H_i(x_2)\right), \tag{70}$$

where $(x_1, x_2) \in [-k_i, 0] \times [-k_i, 0]$.

Considering that $\lambda \cdot \max_{-k_i \le x \le 0}|H_i'(x)| \le 1$, we have

$$\begin{cases} \dfrac{\partial y_1}{\partial x_1} = \dfrac{1}{2}(1 + \lambda H_i'(x)) \ge 0 \\[2mm] \dfrac{\partial y_1}{\partial x_2} = \dfrac{1}{2}(1 - \lambda H_i'(x)) \ge 0. \end{cases} \tag{71}$$

Using that $y_1(0, 0) = 0$ and $y_1(-k_i, -k_i) = -k_i$, then, we have

$$y_1(x_1, x_2) \in [-k_i, 0], \quad (x_1, x_2) \in [-k_i, 0] \times [-k_i, 0].$$

Therefore, if $-k_i \le m_{j+\frac{1}{2}}^{i,n} \le 0$ and $-k_i \le m_{j+\frac{3}{2}}^{i,n} \le 0$, we have

$$-k_i \le m_{j+\frac{1}{2}}^{i,n+1} \le 0, \quad \text{if } j \ne -1, j \ne 0. \tag{72}$$

If $i > 0$ and $j > -1$, the case should be similar.

Then, we estimate $m_{j+\frac{1}{2}}^{i,n+1}$ around the junction point. First, we consider $i < 0$ and $j = -1$

$$m_{-\frac{1}{2}}^{i,n+1} = \frac{m_{-\frac{3}{2}}^{i,n} + m_{-\frac{1}{2}}^{i,n}}{2} - \frac{\lambda}{2}\left(2F_A^n - H_i\left(m_{-\frac{3}{2}}^{i,n}\right) - H_i\left(m_{-\frac{1}{2}}^{i,n}\right)\right). \tag{73}$$

Using that $F_A^n \le 0$, we have

$$m_{-\frac{1}{2}}^{i,n+1} \ge \frac{m_{-\frac{3}{2}}^{i,n} + m_{-\frac{1}{2}}^{i,n}}{2} + \frac{\lambda}{2}\left(H_i\left(m_{-\frac{3}{2}}^{i,n}\right) + H_i\left(m_{-\frac{1}{2}}^{i,n}\right)\right) \tag{74}$$

Set the function

$$y_2 = \frac{1}{2}(x_1 + x_2) + \frac{\lambda}{2}\left(H_i(x_1) + H_i(x_2)\right), \tag{75}$$

where $(x_1, x_2) \in [-k_i, 0] \times [-k_i, 0]$.

Considering that $\lambda \cdot \max_{-k_0 \le x \le 0}|H_i'(x)| \le 1$, we have

$$\begin{cases} \dfrac{\partial y_2}{\partial x_1} = \dfrac{1}{2}(1 + \lambda H_i'(x)) \ge 0 \\[2mm] \dfrac{\partial y_2}{\partial x_2} = \dfrac{1}{2}(1 + \lambda H_i'(x)) \ge 0. \end{cases} \tag{76}$$

Using that $y_2(-k_i, -k_i) = -k_i$, we deduce that

$$y_2(x_1, x_2) \ge -k_i, \quad (x_1, x_2) \in [-k_i, 0] \times [-k_i, 0].$$

Therefore, we have $m_{-\frac{1}{2}}^{i,n+1} \ge -k_i$.

For the second inequality, using that $F_A^n \ge H_j^+\left(m_{-\frac{1}{2}}^{i,n}\right)$, we obtain (77), as shown at the top of the next page. Set the function

$$y_3 = \frac{1}{2}(x_1 + x_2) - \frac{\lambda}{2}\left(2H_i^+(x_2) - H_i(x_1) - H_i(x_2)\right), \tag{78}$$

where $(x_1, x_2) \in [-k_i, 0] \times [-k_i, 0]$.

$$m^{i,n+1}_{-\frac{1}{2}} \leq \frac{m^{i,n}_{-\frac{3}{2}} + m^{i,n}_{-\frac{1}{2}}}{2} - \frac{\lambda}{2}\left(2H^+_i\left(m^{i,n}_{-\frac{1}{2}}\right) - H_i\left(m^{i,n}_{-\frac{3}{2}}\right) - H_i\left(m^{i,n}_{-\frac{1}{2}}\right)\right). \quad (77)$$

Considering that $\lambda \cdot \max_{-k_i \leq x \leq 0} |H'_i(x)| \leq 1$, we have

$$\begin{cases} \dfrac{\partial y_3}{\partial x_1} = \dfrac{1}{2}(1 + \lambda H'_i(x)) \geq 0 \\ \dfrac{\partial y_3}{\partial x_2} = \begin{cases} \dfrac{1}{2}(1 + \lambda H'_i(x)) \geq 0 & -k_i \leq x \leq p_i \\ \dfrac{1}{2}(1 - \lambda H'_i(x)) \geq 0 & p_i \leq x \leq 0 \end{cases} \end{cases} \quad (79)$$

Using that $y_3(0, 0) = 0$, we obtain $m^{i,n+1}_{-\frac{1}{2}} \leq 0$. Thus,

$$-k_i \leq m^{n+1}_{-\frac{1}{2}} \leq 0. \quad (80)$$

Similarly, we estimate the point on the bifurcation lane $i > 0, j > -1$

$$m^{n+1}_{\frac{1}{2}} = \frac{m^n_{\frac{3}{2}} + m^n_{\frac{1}{2}}}{2} - \frac{\lambda}{2}\left(2F^n_A - H_i\left(m^{i,n}_{\frac{3}{2}}\right) - H_i\left(m^{i,n}_{\frac{1}{2}}\right)\right). \quad (81)$$

Using that $F^n_A \leq 0$, $-k_i \leq m^{i,n}_{\frac{3}{2}} \leq 0$ and $-k_i \leq m^{i,n}_{\frac{1}{2}} \leq 0$, we have

$$m^{i,n+1}_{\frac{1}{2}} \leq \frac{m^{i,n}_{\frac{3}{2}} + m^{i,n}_{\frac{1}{2}}}{2} + \frac{\lambda}{2}\left(H_i\left(m^{i,n}_{\frac{3}{2}}\right) + H_i\left(m^{i,n}_{\frac{1}{2}}\right)\right) \leq 0. \quad (82)$$

Using that $F^n_A \geq H^-_i\left(m^{i,n}_{\frac{1}{2}}\right)$, we have

$$\begin{aligned} m^{i,n+1}_{\frac{1}{2}} \geq & \frac{m^{i,n}_{\frac{3}{2}} + m^{i,n}_{\frac{1}{2}}}{2} \\ & + \frac{\lambda}{2}\left(H^-_i\left(m^{i,n}_{\frac{3}{2}}\right) - H_i\left(m^{i,n}_{\frac{3}{2}}\right)\right) \\ & + \frac{\lambda}{2}\left(H^-_i\left(m^{i,n}_{\frac{1}{2}}\right) - H_i\left(m^{i,n}_{\frac{1}{2}}\right)\right) \end{aligned} \quad (83)$$

Set the function

$$y_4 = \frac{1}{2}(x_1 + x_2) + \frac{\lambda}{2}\left(2H^-_i(x_2) - H_i(x_1) - H_i(x_2)\right), \quad (84)$$

where $(x_1, x_2) \in [-k_i, 0] \times [-k_i, 0]$.
Considering that $\lambda \cdot \max_{-k_i \leq x \leq 0} |H'_i(x)| \leq 1$, we have

$$\begin{cases} \dfrac{\partial y_4}{\partial x_1} = \dfrac{1}{2}(1 - \lambda H'(x)) \geq 0 \\ \dfrac{\partial y_4}{\partial x_2} = \begin{cases} \dfrac{1}{2}(1 + \lambda H'_i(x)) \geq 0 & -k_i \leq x \leq p_i \\ \dfrac{1}{2}(1 - \lambda H'_i(x)) \geq 0 & p_i \leq x \leq 0 \end{cases} \end{cases} \quad (85)$$

Using that $y_4(-k_i, -k_i) = -k_i$, we have $m^{i,n+1}_{\frac{1}{2}} \geq -k_i$. Thus,

$$-k_0 \leq m^{i,n+1}_{\frac{1}{2}} \leq 0. \quad (86)$$

□

C. BOUNDARY CONDITIONS FOR HAMILTON-JACOBI SYSTEM

If we want to numerically solve the Hamilton-Jacobi equations with junction conditions, then, suitable boundary conditions are needed. In this subsection, we propose the Dirichlet boundary condition, incoming boundary condition and outgoing boundary condition.

1) DIRICHLET BOUNDARY CONDITION

If the problem setting is that u_x has a compact support in the computational domain, we can set the boundary conditions on the left point as

$$\begin{cases} u^{i,n+1}_{-J} = u^{i,n}_{-J}, \\ u^{i,n+1}_{-J+1} = u^{i,n}_{-J+1}, \end{cases} \quad (87)$$

where x^i_{-J} and x^i_J are artificial/physical boundary points.

The first equation means that there are no other cars coming from the left boundary. The second equation indicates that all the cars will stop at the right boundary one by one. The total amount of traffic in the computational domain will remain unchanged.

2) INCOMING BOUNDARY CONDITION

If there is a stable infinite incoming traffic flow, we set

$$u^i_x(x, t) = M_{f_i}(t), \quad x = -x^i_M. \quad (88)$$

The boundary condition can be Neumann boundary conditions

$$u^i_t + H^+_i(M_{f_i}(t^n)) = 0, \quad x = -x^i_M. \quad (89)$$

Clearly, the above equation is a one-way transmission wave of (6). The total number of incoming cars is $M_{f_i}(t)$. Its numerical discretization is

$$\frac{u^{i,n+1}_{-J} - u^{i,n}_{-J}}{\Delta t} + H^+_i(M_{f_i}(t)) = 0 \quad (90)$$

3) OUTGOING BOUNDARY CONDITION

As we present above, if the right boundary is written as the Dirichlet boundary condition, then, all the cars will stop at the right boundary. If we want, all the cars are free to exit the computational domain, just as there is no right boundary.

The outgoing boundary condition is written as

$$u^i_t + H^-_i(u^i_x) = 0, \quad x = x^i_M, \quad (91)$$

and its numerical discretization is

$$\frac{u_j^{i,n+1} - u_j^{i,n}}{\Delta t} + H_i^-(\frac{u_j^{i,n} - u_{j-1}^{i,n}}{\Delta x}) = 0. \tag{92}$$

To summarize, for simulating traffic flow networks, we solve Hamilton-Jacobi equations with some junction conditions. We present a finite difference scheme Eq. (59) with a numerical junction condition Eq. (64), some suitable initial data and the boundary conditions Eq. (87), Eq. (90) or Eq. (92). In the next section, we will test this scheme numerically.

IV. NUMERICAL VALIDATION AND APPLICATION

In this section, we verify the validity of the junction conditions proposed above and apply the local perturbation problem to a traffic light problem.

A. LOCAL PERTURBATION AND INFLUENCE OF THE FLUX LIMITER A

First, we test the local perturbation problem.

Based on the previous work [30], we assume the following numerical test and set the related parameters are as follows:

$$x_M = 200, \quad J = 2000, \ \Delta x = \frac{x_M}{J} = 0.1, \ \Delta t = 0.001.$$

We consider a Greenshields optimal velocity function:

$$V(h) = \begin{cases} 0 & h \leq h_0, \\ V_{max}\left(1 - \left(\frac{h_0}{h}\right)^2\right) & h_0 < h < h_{max}, \\ V_{max}\left(1 - \left(\frac{h_0}{h_{max}}\right)^2\right) & h > h_{max}. \end{cases} \tag{93}$$

For the values of the different parameters for the optimal velocity function, we take

$$\begin{cases} V_{max}^{-1} = V_{max}^1 = 58\text{km/h}, \\ h_0^{-1} = h_0^1 = 2\text{m}, \\ h_{max}^{-1} = h_{max}^1 = 25\text{m}. \end{cases} \tag{94}$$

Therefor, we can calculate the function H_i with the following parameters:

$$\begin{cases} k_{-1} = k_1 = 0.5\text{m}^{-1}, \\ p_{-1} = p_1 = -0.25\text{m}^{-1}, \\ H_{-1}(p_{-1}) = H_1(p_1) = -2.0139\text{s}^{-1}. \end{cases} \tag{95}$$

In our setting, we have

$$\max_u \left(|H'_{-1,1}(u_x)|\right) \leq 16. \tag{96}$$

Thus, the time step $\Delta t = 0.01$ fits the CFL condition (60). First, we study a Gaussian beam packet

$$u(x,0) = u_0(x) = \int_{-x_M}^x \left(-U * \exp\left(-b(y - x_1)^2\right)\right) dy$$

going across the local perturbation point $x = 0$ (see Figs. 6 to 11), where $U = 0.75k_0$, $b = 0.008$, and $x_1 = -50$. We set
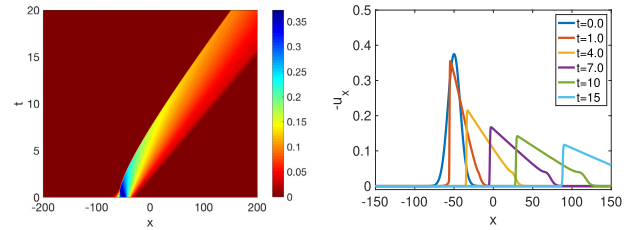

FIGURE 6. The time evolution of density $(-u_x(x,t))$ without local perturbation.
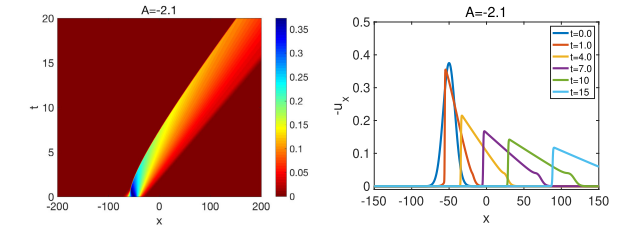

FIGURE 7. The time evolution of density $(-u_x(x,t))$ with the flux limiter $A = -2.1$.
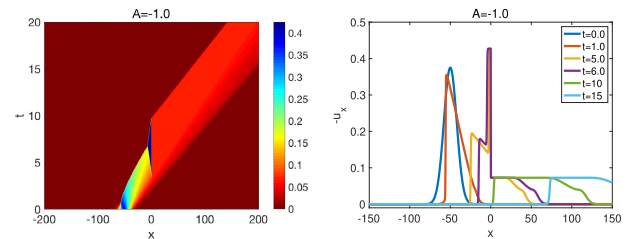

FIGURE 8. The time evolution of density $(-u_x(x,t))$ with a different flux limiter $A = -1.0$.

the left boundary condition as the Dirichlet boundary condition (87) and the right boundary condition as the outgoing boundary condition (92).

Here, Fig. 6 shows the system without local perturbation, and Figs. 7 to 11 show the system with local perturbation which in the flux limiter is $A = -2.1, -1.0, -0.5, -0.1, 0$, respectively. From these figures, we find the following

- When there is no perturbation point, the wave packet moves forward. A shock wave (discontinuity) is generated at the rear of the Gaussian wave packet. This is due to the rear of the wave packet having a small traffic density and fast speed, while the centre of the wave packet has a high traffic density and slow speed. After such a nonlinear interaction, the shock wave is produced.
- When $A \leq A_0$, the flux limiter does not work, and the system is strictly similar to the one obtained without a local perturbation.
- When $A = -1$, the flux limiter begins to show its blocking effect on traffic.
- When A continues to increase to -0.5, the blocking effect of the limiter on the traffic flow becomes more pronounced. The time for which the entire flow has crossed the perturbation point is significantly increased.
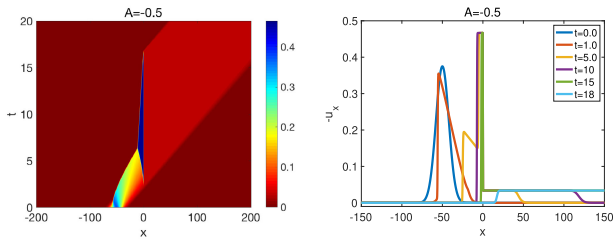
FIGURE 9. The time evolution of density $(-u_x(x, t))$ with a different flux limiter $A = -0.5$.
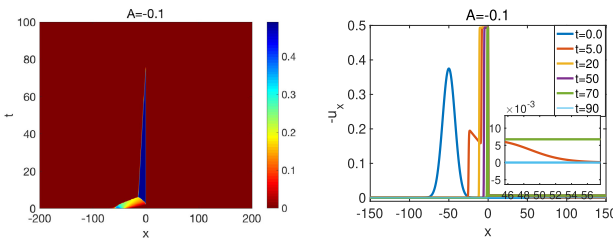

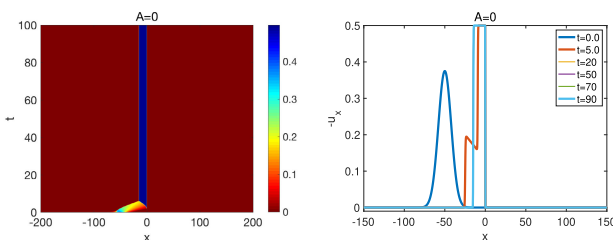**FIGURE 10.** The time evolution of density $(-u_x(x, t))$ with a different flux limiter $A = -0.1$.

FIGURE 11. The time evolution of density $(-u_x(x, t))$ with a different flux limiter $A = 0$.

TABLE 1. Block data with different flux limiter *A*.

Flux limiter A	-2.1	-1	-0.5	-0.1	0
Block time(start)	-	3.1	2.35	1.82	1.45
Time to max density(start)	-	5.6	4.30	3.6	2.6
Block time(end)	-	9.55	16.6	75.5	∞
Blocking time length	-	6.45	14.25	73.86	∞
max density before junction	-	0.425	0.47	0.495	0.5
max density after junction	-	0.075	0.04	0.006	0

- When A is infinitely close to 0, such as $A = -0.1$, the traffic is blocked behind the origin point, only allowing traffic to pass at an extremely slow speed.
- When $A = 0$, the flux limiter can block the entire flow. Just as at the crossroads, the traffic was blocked by the red light.

We list some block data caused by different flux limiters A. From Table 1, we have the following observations as the flux limiter A increases:

- The time to retardation and that to maximum density are shortened. The time that the traffic flow is blocked also increases.
- The maximum density before the junction increases. When it reaches its maximum, all cars nearly stop before the junction.
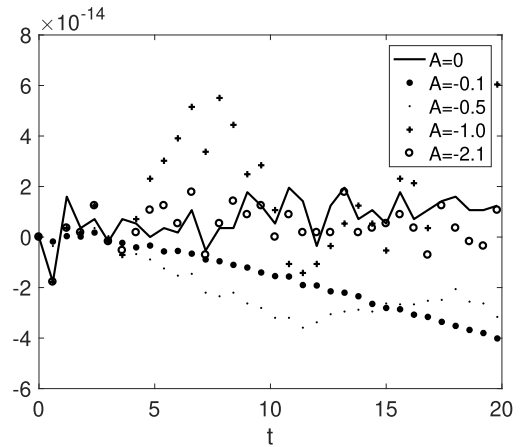- The density after the junction gradually decreases.

FIGURE 12. Time evolution of relative error $\varepsilon(t)$.

Third, we study the conservation of the cars and some other attributes for the numerical method. In this part, we change the right boundary to a Dirichlet boundary condition. Fig. 12 shows the total number of cars. We define the total traffic number as

$$I(t) = \int_{x_r}^{x_l} (-u_x(x, t)) dx, \tag{97}$$

and the relative error in time as

$$\varepsilon(t) = \frac{I(t) - I(0)}{I(0)}. \tag{98}$$

Fig. 12 shows the relative error of the total traffic number. From this and the above figures, we can observe the following

- The total number of cars is almost unchanged. The relative error is approximately 10^{-14}, which means that our algorithm is very good at retaining the conservation of traffic flow.
- The value of density $(-u_x)$ is still non-negative irrespective of A in our calculation interval. Moreover, the traffic density is always in $[0, 0.5]$. The numerical method also maintains this property.

B. APPLICATION TO TRAFFIC LIGHTS
In this part, we will present one application of this model: the modelling of traffic lights. We considered the traffic lights on the crossroad to be a time-dependent flux limiter such as

$$A(t) = \begin{cases} 0 & t \mod 10 \in [0, 6], \\ H(p_0) & t \mod 10 \in [6, 10). \end{cases} \tag{99}$$

Fig. 13 shows the time-dependent flux limiter $A(t)$ in the traffic simulation with traffic lights. As shown, we assume that there is a red traffic light that is active when $A(t) = 0$, while the green traffic light is active when $A(t) = H(p_0)$. The computational domain that we set is $[-150, 150]$. The left boundary condition is the incoming boundary condition $M_f(t)$ that reads as
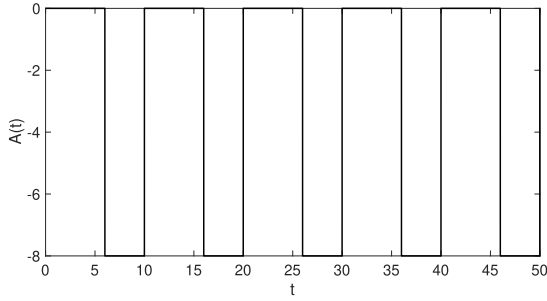
$$M_f(t) = \alpha(\sin(\omega t))^2, \tag{100}$$

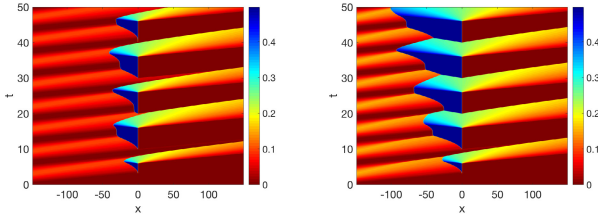**FIGURE 13.** The flux limiter $A(t)$ in the traffic light simulation.

FIGURE 14. The time evolution in the traffic light simulation with parameters $\alpha_1 = 0.1$ (left) and $\alpha_2 = 0.15$ (right).

and we set the right boundary as the outgoing boundary condition.

Here, we set $\omega = 0.5$ and set α as 0.1 and 0.15. The results are shown in Fig. 14.

From these figures, we find the following

- In each cycle, the traffic is blocked and released when traffic lights (red/green) appear alternately.
- This traffic system with these traffic lights is suitable for $\alpha = 0.1$, while it is not suitable for $\alpha = 0.15$. The cars will increasingly accumulate behind the traffic light when $\alpha = 0.15$.
- Clearly, our approach can be used to optimize and simulate traffic flows in the case of traffic lights.

C. NUMERICAL VALIDATION FOR BIFURCATION CONDITION

In this subsection, we will only show the effectiveness of the junction conditions. First, we test the bifurcation condition.

In this test, we select $M = 1$ and $N = 3$. Four lanes have the Greenshields optimal velocity functions as Eq.(93). The max velocities for the lanes are

$$\begin{cases} V_{max}^0 = 120\text{km/h}, & V_{max}^1 = 120\text{km/h}, \\ V_{max}^2 = 70\text{km/h}, & V_{max}^3 = 58\text{km/h}. \end{cases}$$

The bifurcation coefficients are

$$\beta_1 = 0.4, \quad \beta_2 = 0.4, \ \beta_3 = 0.2.$$

Additionally the flux limiter is $A = -2$.

The computational domain is defined on

$$\begin{aligned} \mathbf{J}_0 &= [-300, 0] \cdot \mathbf{e}^0, \\ \mathbf{J}_i &= [0, 300] \cdot \mathbf{e}^i, \quad i = 1, 2, 3. \end{aligned} \quad (101)$$
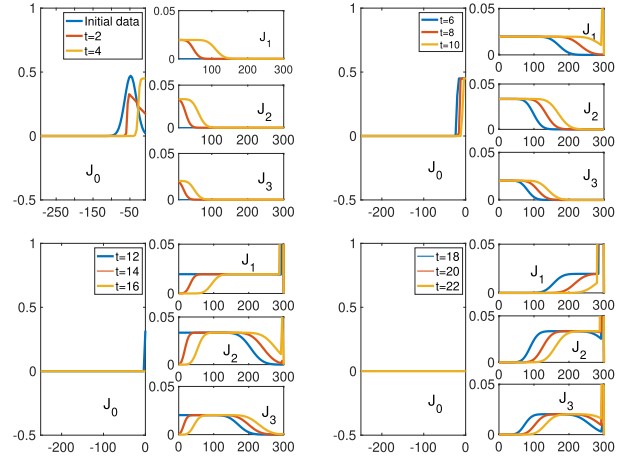

FIGURE 15. The time evolution of density $(-u_x(x, t))$ for the bifurcation problem with parameters $\beta_1 = 0.4$, $\beta_2 = 0.4$, $\beta_3 = 0.2$ and $V_{max}^0 = 120\text{km/h}$, $V_{max}^1 = 120\text{km/h}$, $V_{max}^2 = 70\text{km/h}$, $V_{max}^3 = 58\text{km/h}$.
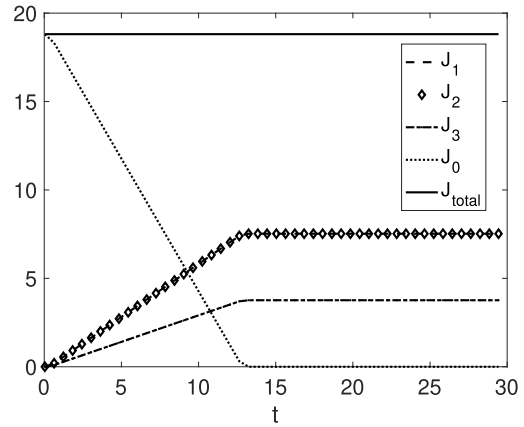

FIGURE 16. The number on each lane against t for the bifurcation problem.

The initial data are a Gaussian beam in $\mathbf{J}_0$

$$u(x, 0) = \int_{-300}^{x} \left(0.475 * \exp\left(-0.002(y+50)^2 \right) \right) dy, \quad (102)$$

and $u(x, 0) = 0$ on $\mathbf{J}_i, i = 1, 2, 3$. Both left and right boundary conditions can be selected as Dirichlet boundary conditions. The discretization parameters $\Delta x = 1$ and $\Delta t = 0.01$ fit the CFL condition (60).

The result is shown in Fig. 15 which reveals the following:

- All cars flow into three lanes at the junction point.
- The traffic was slightly blocked at the junction point by the flux limiter A.
- Finally, all cars enter the three-lane lane with the given rate $\beta_i, i = 1, 2, 3$.

The curves of the total number of each lane over time are shown in Fig. 16. We observe the following:

- The total number of all lanes is strictly unchanged.
- The numbers of cars on $\mathbf{J}_1$ and $\mathbf{J}_2$ are always the same and twice the number of cars on $\mathbf{J}_3$.

Here, we should note that the total number being unchanged is very important. This linked the stability of the Hamilton-Jacobi system.
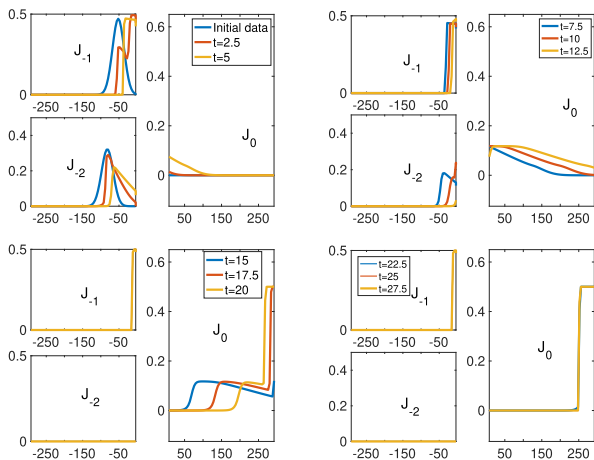
FIGURE 17. The time evolution of density $(-u_x(x, t))$ for the merging problem with parameters $\alpha_1 = 0.5$, $\alpha_2 = 0.5$ and $V_{max}^{-1} = 120$km/h, $V_{max}^{-2} = 120$km/h, and $V_{max}^{0} = 58$km/h.
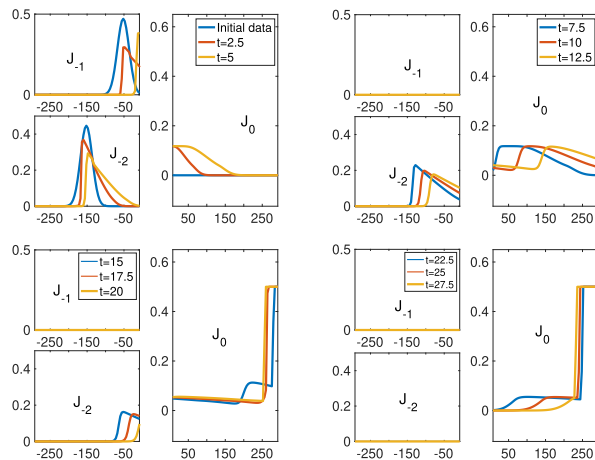

FIGURE 19. The time evolution of density $(-u_x(x, t))$ for the merging problem without certain merging parameters and $V_{max}^{-1} = 120$km/h, $V_{max}^{-2} = 58$km/h, and $V_{max}^{0} = 120$km/h.
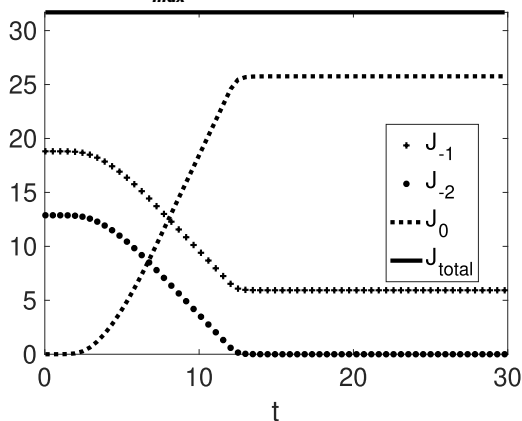

FIGURE 18. The number on each lane against t for the merging problem with certain merging parameters.
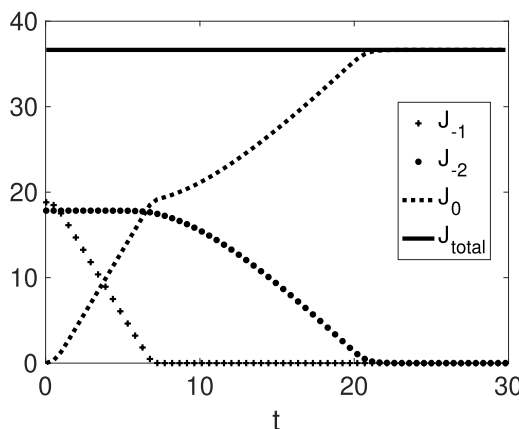

FIGURE 20. The number on each lane against t for the merging problem without certain parameters.

D. NUMERICAL VALIDATION FOR MERGING CONDITION

Then, we test the merging condition.

First, we test the process of merging ($M = 2$ and $N = 1$) by a given percentage $\beta_1 = \beta_2 = 0.5$ as a zipper. The max velocities for the lanes are

$$V_{max}^{-1} = 120\text{km/h}, \quad V_{max}^{-2} = 120\text{km/h}, \quad V_{max}^{0} = 70\text{km/h}.$$

and $A = -2$.

The computational domain is defined on

$$\mathbf{J}_i = [-300, 0] \cdot \mathbf{e}^i, \quad i = -1, -2,$$
$$\mathbf{J}_0 = [0.300] \cdot \mathbf{e}^0. \quad (103)$$

We set nonzero initial data on both lanes $\mathbf{J}_{-1}$ and $\mathbf{J}_{-2}$.

$$u(x, 0) = \int_{-300}^{x} \left(0.475 * \exp\left(-0.002(y + 50)^2 \right) \right) dy, \quad (104)$$

and

$$u(x, 0) = \int_{-300}^{x} \left(0.325 * \exp\left(-0.002(y + 80)^2 \right) \right) dy, \quad (105)$$

respectively. The boundary condition and discretization parameters are the same as in the above subsection.

The result is shown in Fig. 17 and Fig. 18, which show the following:

- The two traffic streams flow into $\mathbf{J}_0$ at the junction point.
- The traffic was slightly blocked at the junction point by the flux limiter A.
- The total numbers of all lanes are strictly unchanged.
- Due to the different numbers of $\mathbf{J}_{-1}$ and $\mathbf{J}_{-2}$, there are still some cars on $\mathbf{J}_{-1}$ after all the cars go away from $\mathbf{J}_{-2}$. The remaining cars on $\mathbf{J}_{-1}$ will be stuck at the junction point forever.

Then, we tested the next merging junction condition. The other conditions remain unchanged. We only change the initial value on $\mathbf{J}_{-2}$

$$u(x, 0) = \int_{-300}^{x} \left(0.325 * \exp\left(-0.002(y + 150)^2 \right) \right) dy. \quad (106)$$

The result is changed to Fig. 19 and Fig. 20. Some aspect has changed because

- The traffic no longer remitted in accordance with a fixed proportion but in accordance with the current flow of merging.
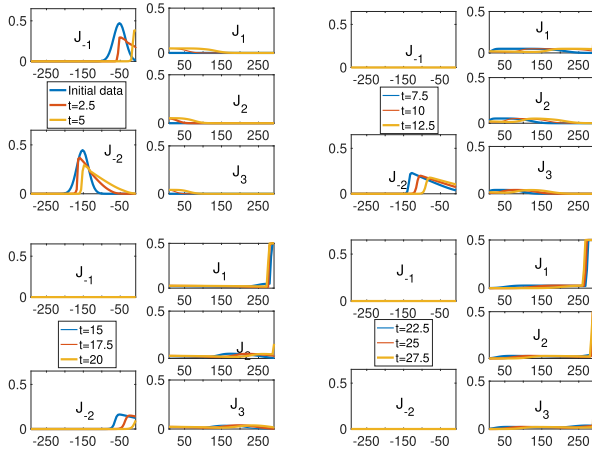
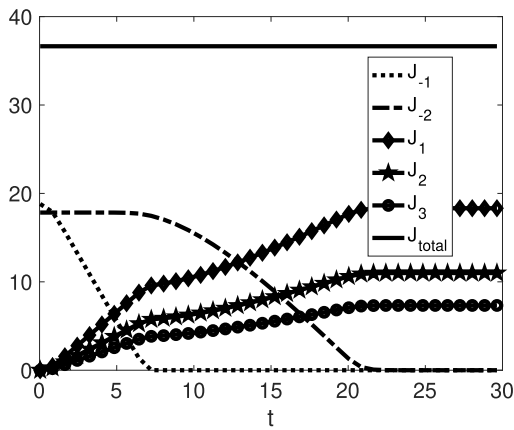**FIGURE 21.** The time evolution of a real *M*-in-*N*-out problem.

FIGURE 22. The number on each lane against *t*.

- By the time that $t = 7$, the traffic on $\mathbf{J}_{-1}$ had already left. However, the cars on $\mathbf{J}_{-2}$ can still continue to enter $\mathbf{J}_0$ until $t = 22$.

E. NUMERICAL VALIDATION FOR MULTI-IN-MULTI-OUT CONDITION

We turn to an *M*-in-*N*-out numerical problem in this subsection.

In this part, we select $M = 2$ and $N = 3$. We combine the above two subsections that in which the nonzero initial data are on $\mathbf{J}_{-1}$ and $\mathbf{J}_{-2}$. Every condition is unchanged.

A real *M*-in-*N*-out numerical problem is shown in Fig. 21 and Fig. 22, which show the following:

- The merging flow goes into the junction point according to the proportion of the flux.
- The traffic flows into $\mathbf{J}_i$, $i = 1, 2, 3$ according to a certain percentage.
- The total number of vehicles is strictly unchanged.

F. APPLICATION TO INTERSECTION WITH MEASURED DATA

To further verify the validity of the model and calculation method proposed in this paper, we acquired the measured
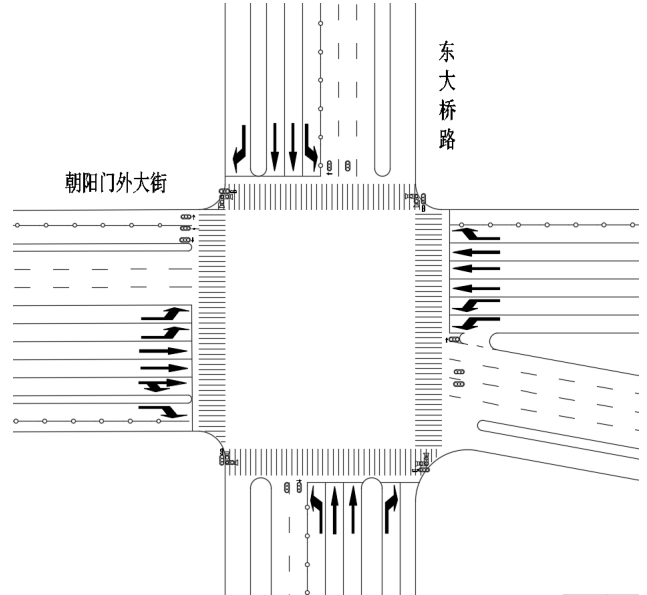

FIGURE 23. Diagram of the intersection of Chaoyangmenwai Street and Dongdaqiao Road.

TABLE 2. Timing status of traffic lights within a time period *T* = 206s.

Phase	Straight North-South	Turn left from North to South	Eastern one-sided
Time	47 s	33 s	17 s
Phase	Straight East-West	Motor Vehicles to East and West	Turn left from East to West
Time	52 s	27 s	30 s

data from videos recorded near the intersection of Chaoyangmenwai Street and Dongdaqiao Road in Beijing (these data were provided by Kyland Technology Company), and then we performed numerical simulations using these data.

The east-west direction is Chaoyangmenwai Street, and the north-south direction is Dongdaqiao Road. There are four left-turn arrow lights, one direct signal light, one right-turn signal light and four round-headed lights (a total of ten lights) in this intersection. The open and close mode of the signal lamp is shown in this section, part B. The traffic lights are controlled by multi-period periodic control. There is no green wave control on the main road. The timing of the signal lamp is shown in Table 2. The left-turn node is affected by the direct traffic flow; thus, it is necessary to design the flow restriction conditions separately.

We have traffic flow detectors at four entrances (turn left, turn right and go straight). The values enter the incoming boundary conditions used by the Hamilton-Jacobi equation. The lanes in the four exit directions are set as the outgoing boundary conditions.

One of the most important values that we are concerned with at the intersection is the number of cars in the queue. To study the number of queued cars, we take one hour for the numerical simulation of early peak 7:30-8:30, peak 14:00-15:00 and evening peak 17:30-18:30 on June 29, 2019. We record the maximum number of queued cars at the

TABLE 3. Comparison of observation and numerical results of maximum queue length at intersections (relative error shown in parentheses).

	Early Peak Time		Peak Time		Evening Peak Time	
	Observation Results	Numerical Results	Observation Results	Numerical Results	Observation Results	Numerical Results
East Entrance	19	17 (-10.5%)	15	14 (-6.67%)	18	19 (5.56%)
South Entrance	17	17 (0%)	16	14 (12.5%)	17	16 (-5.88%)
West Entrance	22	25 (13.6%)	23	24 (4.3%)	25	28 (12.0%)
North Entrance	16	17 (6.25%)	15	16 (6.67%)	21	24 (14.2%)

intersection and compare it with the results of video traffic photographs, as shown in Table 3.

The above table shows that the numerical results are in good agreement with the actual data collected by video. The overall relative error is within ±15%. The largest relative error occurs during the evening peak of the north entrance, which is 14.2%, and the smallest occurs during the early peak time of the south entrance. This result means that the results of this model have high accuracy both qualitatively and quantitatively. The model proposed in this paper is suitable for studying the problem of traffic flows at such junctions.

V. CONCLUSION

Based on the first-order car-following model in a traffic network, we use a new macroscopic traffic flow model to simulate the traffic network. The model is described by a set of PDEs plus a junction condition. The junction condition provides the distribution rules of the roads and is often with a flux limiter. We analytically studied junction conditions. Then, we studied a numerical method for computing this system. Finally, we studied the traffic junction numerically and demonstrated its effectiveness.

The main contributions of this paper are as follows:

- Junction conditions for local perturbation, bifurcation and merging are proposed;
- Furthermore, the real traffic junction condition (M-in-N-out) is also proposed;
- An effective numerical method for computing the Hamilton-Jacobi equations with junction conditions is proposed;
- The Dirichlet boundary condition, incoming boundary condition and outgoing boundary condition are proposed;
- The boundedness, regularity and conservation of this numerical method are proven;
- The influence of flux limiter in traffic flows is studied;
- Numerical studies are presented to demonstrate the effectiveness of the conditions.

AUTHORS' CONTRIBUTIONS

Mrs. Linfeng Zhang designed the junction conditions and numerical methods for Hamilton-Jacobi systems in Professor Nicolas Forcadel's lab when she visited the INSA of Rouen, France. She finished writing Sections 2,3 and 4 in Professor Bin Ran's lab when she visited the University of Wisconsin-Madison. Professor Hongfei Jia and Professor Bin Ran wrote the introduction section and revised Section 3 and 4, provided valuable suggestions and supervised the whole work. Professor Nicolas Forcadel performed the PDE analysis of the Hamilton-Jacobi system and read and revised the entire manuscript. All authors read and approved the final manuscript.

REFERENCES

[1] D. Chowdhury, L. Santen, and A. Schadschneider, "Statistical physics of vehicular traffic and some related systems," *Phys. Rep.*, vol. 329, nos. 4–9, pp. 199–329, May 2000.

[2] D. Helbing, "Traffic and related self-driven many-particle systems," *Rev. Mod. Phys.*, vol. 73, no. 4, p. 1067, 2001.

[3] M. J. Lighthill and G. B. Whitham, "On kinematic waves. II. A theory of traffic flow on long crowded roads," *Proc. Roy. Soc. London, Ser. A, Math. Phys. Sci.*, vol. 229, no. 1178, pp. 317–345, 1955.

[4] P. I. Richards, "Shock waves on the highway," *Oper. Res.*, vol. 4, no. 1, pp. 42–51, 1956.

[5] M. Garavello and B. Piccoli, *Traffic Flow on Networks*. Springfield, MO, USA: American Institute of Mathematical Sciences, 2006.

[6] G. F. Newell, "A simplified theory of kinematic waves in highway traffic, part I: General theory," *Transp. Res. B, Methodol.*, vol. 27, no. 4, pp. 281–287, Aug. 1993.

[7] C. Imbert and R. Monneau, "Flux-limited solutions for quasi-convex Hamilton–Jacobi equations on networks," *Ann. Sci. Éc. Norm. Supér.*, vol. 50, no. 2, pp. 357–448, 2017.

[8] L. A. Pipes, "An operational analysis of traffic dynamics," *J. Appl. Phys.*, vol. 24, no. 3, pp. 274–281, 1953.

[9] M. Brackstone and M. McDonald, "Car-following: A historical review," *Transp. Res. F, Traffic Psychol. Behav.*, vol. 2, no. 4, pp. 181–196, Dec. 1999.

[10] E. Kometani and T. Sasaki, "On the stability of traffic flow (report-I)," *J. Oper. Res. Soc. Jpn.*, vol. 2, no. 1, pp. 11–26, 1958.

[11] D. C. Gazis, R. Herman, and R. W. Rothery, "Nonlinear follow-the-leader models of traffic flow," *Oper. Res.*, vol. 9, no. 4, p. 545–567, 1961.

[12] P. G. Gipps, "A behavioural car-following model for computer simulation," *Transp. Res. B, Methodol.*, vol. 15, no. 2, pp. 105–111, 1981.

[13] M. Bando, K. Hasebe, A. Nakayama, A. Shibata, and Y. Sugiyama, "Dynamical model of traffic congestion and numerical simulation," *Phys. Rev. E, Stat. Phys. Plasmas Fluids Relat. Interdiscip. Top.*, vol. 51, no. 2, p. 1035, 1995.

[14] C. F. Daganzo, "The cell transmission model: A dynamic representation of highway traffic consistent with the hydrodynamic theory," *Transp. Res. Part B, Methodol.*, vol. 28, no. 4, pp. 269–287, Aug. 1994.

[15] C. F. Daganzo, "The cell transmission model, part II: Network traffic," *Transp. Res. B, Methodol.*, vol. 29, no. 2, pp. 79–93, 1995.

[16] I. Yperman, S. Logghe, C. M. Tampere, and B. Immers, "Multicommodity link transmission model for dynamic network loading," in *Proc. 85th Annu. Meeting Transp. Res. Board*, Washington, DC, USA, 2006.

[17] I. Yperman, "The link transmission model for dynamic network loading," Ph.D. dissertation, Katholieke Univ. Leuven, Leuven, Belgium, Jun. 2007. [Online]. Available: https://lirias.kuleuven.be/1749225?limo=0

[18] L. Fermo and A. Tosin, "A fully-discrete-state kinetic theory approach to modeling vehicular traffic," *SIAM J. Appl. Math.*, vol. 73, no. 4, pp. 1533–1556, 2013.

[19] N. Bellomo and C. Dogbe, "On the modeling of traffic and crowds: A survey of models, speculations, and perspectives," *SIAM Rev.*, vol. 53, no. 3, pp. 409–463, 2011.

[20] Y. Li, C. G. Claudel, B. Piccoli, and D. B. Work, "A convex formulation of traffic dynamics on transportation networks," *SIAM J. Appl. Math.*, vol. 77, no. 4, pp. 1493–1515, 2017.

[21] S. Osher and C.-W. Shu, "High-order essentially nonoscillatory schemes for Hamilton–Jacobi equations," *SIAM J. Numer. Anal.*, vol. 28, no. 4, pp. 907–922, 1991.

[22] G.-S. Jiang and C.-W. Shu, "Efficient implementation of weighted ENO schemes," *J. Comput. Phys.*, vol. 126, no. 1, pp. 202–228, Jun. 1996.

[23] S. Göttlich, U. Ziegler, and M. Herty, "Numerical discretization of Hamilton–Jacobi equations on networks," *Proc. NHM*, vol. 8, no. 3, pp. 685–705, 2013.

[24] E. Carlini, A. Festa, and N. Forcadel, "A semi-Lagrangian scheme for Hamilton–Jacobi equations on networks with application to traffic flow models," 2018, *arXiv:1804.09429*. [Online]. Available: https://arxiv.org/abs/1804.09429

[25] N. Forcadel, W. Salazar, and M. Zaydan, "A junction condition by specified homogenization of a discrete model with a local perturbation and application to traffic flow," *Commun. Pure Appl. Anal.*, vol. 17, no. 5, pp. 2173–2206, 2018.

[26] G. Costeseque, J.-P. Lebacque, and R. Monneau, "A convergent scheme for Hamilton–Jacobi equations on a junction: Application to traffic," *Numer. Math.*, vol. 129, no. 3, pp. 405–447, Mar. 2015.

[27] J. Guerand and M. Koumaiha, "Error estimates for finite difference schemes associated with Hamilton–Jacobi equations on a junction," Jun. 2017, *arXiv:1502.07158*. [Online]. Available: https://arxiv.org/abs/1502.07158

[28] C. Imbert, R. Monneau, and H. Zidani, "A Hamilton–Jacobi approach to junction problems and application to traffic flows," *ESAIM, Control, Optim. Calculus Variat.*, vol. 19, no. 1, pp. 129–166, Jan. 2013.

[29] C. Imbert and R. Monneau, "Flux-limited solutions for quasi-convex Hamilton–Jacobi equations on networks," 2013, *arXiv:1306.2428*. [Online]. Available: https://arxiv.org/abs/1306.2428

[30] W. Salazar, "Numerical specified homogenization of a discrete model with a local perturbation and application to traffic flow," *ANZIAM J.*, vol. 59, pp. 50–97, May 2017.
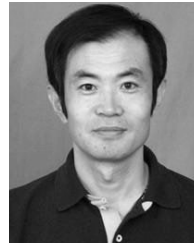
HONGFEI JIA was born in Shandong, China. He received the Ph.D. degree in transportation from Jilin University, where he is currently a Full Professor, a Doctoral Supervisor, and a Transportation Engineering Expert. He has been involved in research and pedestrian flow, traffic flow, automatic vehicles, and traffic management.

NICOLAS FORCADEL received the Ph.D. degree from the l'ENPC et a l'Université de Marne la Valleé, in 2007. Then, he completed the Post-doctoral Research at the l'équipe Commadns de l'INRIA Saclay Ile de France. He is currently a Full Professor with the Institut National de Sciences Appliquées (INSA) of Rouen. His research interests include optimal control, homogenization of nonlinear Hamilton–Jacobi equations, nonlinear equations with non-local terms, convergence and error estimates for numerical scheme, fast marching method, dislocations dynamics, and traffic modeling.

LINFENG ZHANG received the B.S. degree from Heilongjiang University, in 2009. She is currently pursuing the Ph.D. degree in transportation management engineering with Jilin University.

She was a Visiting Scholar with the Insititut National de Sciences Appliquees (INSA) of Rouen, France, from January to August 2017, and the University of Wisconsin–Madison during her Ph.D. study funded by the China Scholarship Council. Her research interests include numerical analysis, traffic flow simulation, fluid mechanics, numerical PDE, CAVH, and big-data analysis.

BIN RAN is currently a Vilas Distinguished Achievement Professor with the University of Wisconsin–Madison, Madison, WI, USA. He is also an Expert in dynamic transportation network models, traffic simulation and control, traffic information systems, and connected automated vehicle highway (CAVH). He has led the development and deployment of various traffic information systems and technologies in USA and China. He has trained younger generations of professors and experts in traffic engineering and intelligent transportation systems (ITS) in USA, China, South Korea, and other countries. He has authored two leading textbooks on dynamic traffic networks. He has coauthored more than 180 journal papers and more than 240 referenced papers at national and international conferences. He has coauthored six books on intelligent highways in China. He holds three U.S. patents and 12 Chinese patents and has more than a dozen patents pending in USA, China, and PCT. His research has focused on five major areas, such as intelligent transportation system (ITS) technology development and system evaluation, dynamic transportation network and traffic modeling, development of mobile probe technologies for traffic state estimation and passenger flow estimation, connected automated vehicle highway (CAVH), vehicle highway coordination, intelligent vehicles, and automated highway systems, and big-data applications for multi-modal transportation databases.

● ● ●